Uplift Resistance Capacity of Anchor Piles used in Marine Aquaculture

Fukun Gui
Zhejiang Ocean University
Jianqiao Kong
Zhejiang Ocean University
Dejun Feng
Zhejiang Ocean University
Xiaoyu Qu (quxiaoyu@zjou.edu.cn)
Zhejiang Ocean University
Fang Zhu
Zhejiang Ocean University
Yang You
Zhejiang Ocean University

Research Article

Keywords: Anchor Piles , Marine Aquaculture, harsh ocean environments

Posted Date: June 24th, 2021

DOI: https://doi.org/10.21203/rs.3.rs-640464/v1

Uplift resistance capacity of anchor piles used in marine aquaculture

Fukun Gui[1], Jianqiao Kong[1], Dejun Feng[1], Xiaoyu Qu[2,*], Fang Zhu[1], and Yang You[1]

[1]National Engineering Research Center for Marine Aquaculture, Zhejiang Ocean University, Zhoushan, 316022, China
[2]School of Fisheries, Zhejiang Ocean University, Zhoushan, 316022, China
[*]corresponding.author quxiaoyu@zjou.edu.cn
[+]these authors contributed equally to this work

ABSTRACT

Anchor piles are widely used in marine aquaculture, and their uplift resistance capacity largely determines their safety, especially in harsh ocean environments. However, a practical guide on its design and installation is wanting. Laboratory experiments were conducted to investigate the effect of the initial tension angle, pile diameter, embedded depth, and pile configuration on the uplift resistance capacity of anchor piles for marine aquaculture under oblique loads. The results show that increasing the initial tension angle of circular and square single piles can significantly improve the uplift resistance capacity. The failure load of the square single pile was slightly higher than that of the circular single pile. Increasing the pile diameter can effectively improve the failure load and delay the development speed of the pile top displacement. Increasing the embedded depth can effectively improve the failure load and increase the lateral displacement of the pile top. The uplift resistance capacity of the dual anchor piles was better than that of the single anchor piles. The layout configuration has little effect on the failure load, but has a large effect on the dis-placement development.

Introduction

Net cage and longline aquaculture are two common marine aquaculture methods. The China Fishery Statistical Yearbook shows that in 2019, the fishery output of these two aquaculture methods reached more than 690,000 tons, accounting for 33.5% of China's total marine aquaculture production[1].Anchors form an important part of the mooring system and directly affect the safety and stability of marine aquaculture equipment. The conventional gravity concrete anchors used in marine aquaculture easily deviate, making it difficult to fix the anchoring position. Anchor piles, as simple structures and low-cost anchors, are widely used in net cage and longline aquaculture and provide accurate positioning and difficult-to-change anchor post positions (Figure 1). The anchor piles used in marine aquaculture mainly bear the effect of an oblique tension load[2],with a complicated interaction occurring between the anchor piles and the soil. At present, because of the scarcity of relevant research, a practical guide on the design and installation of anchor piles is lacking. Therefore, guaranteeing the safety and stability of aquaculture equipment difficult. As such, conducting research on the uplift resistance capacity of anchor piles is of great significance for marine aquaculture.

Presently, studies on the uplift resistance capacity of anchors used in marine aqua-culture have been established based on crude assumptions. Trujillo et al.[3] conducted tests on different types of deadweight anchors commonly used in longline aquaculture, suggesting possible differences as a function of different tension angles. Cortes-Garcia et al.[2] used finite element analyses to illustrate the capacity of the helical anchor for oblique loads, explored the suitability of applying helical anchors to aquaculture equipment, and concluded that helical anchors are more suitable for tensioned mooring. Hou et al.[4] used the lumped-mass method to study the effect of embedded anchor chains on the dynamic characteristics of aquaculture net cages. The study of applying uplift resistance to anchor members has matured in another field engineering[5]. Rao et al.[6] and Esfeh et al.[7] used model experiments and numerical simulations to study the uplift resistance capacity of suction piles. Wang et al.[8] and Kwon et al.[9] used centrifuge model experiments and finite element analysis to study the uplift resistance of helical anchors. Yi et al.[10] used finite element analysis to study the uplift resistance capacity and failure envelopes of torpedo anchors embedded off-verticality. However, the most of the anchors mentioned are used in offshore structures such as offshore drilling platforms, and the designed water depth is not less than 100 m. The current design water depth of marine aquaculture engineering equipment is generally within 50 m[11], and the above research results cannot be directly applied to marine aquaculture engineering equipment.

Pile foundations are widely used in onshore engineering and considerable research on pile foundations under oblique loads exists. generally, the research methods to de-compose the oblique load into lateral and vertical loads on the pile foundation. Ayothiraman et al.[12] and Reddy et al.[13] conducted uplift laboratory model experiments with and without a lateral load, respectively. Their research found that compared with the case of no lateral load, the failure load increased in the case of lateral load, and the displacement and deflection of the pile top also increased significantly. Conte et al.[14] fully considered the occurrence of plastic strains in the soil, concrete cracking and steel yielding in the pile as well as the occurrence of slip and gap at the pile–soil interface, and proposed a new constitutive model that can simulate the bearing performance of a flexible long pile foundation under different inclination angles. This simplified analysis method does not fully consider the coupling effect of combined loads. Other researchers take the oblique load be directly placed on the pile. Lu et al.[15] used a centrifuge experiment to impose an oblique load on the model pile and found that as the horizontal load increased, the bending moment of the pile first de-creased and then increased. The additional settlement of the pile was caused by the horizontal load and was positively related to the vertical load, that is, the "P-Δ" effect. Achmus et al.[16] established a numerical system that can clearly describe the interactions of the pile and solid and their quantitative importance and studied the effects of different factors on the action of combined loads. Shin et al.[17] applied the different directions of the uplift load of a rigid metal model in a compacted near-saturated clay soil and proposed an empirical formula for the relationship between the load inclination angle and the failure load. Yang et al.[18] in laboratory uplift model experiments, found that after the failure of the pile under the oblique load, the soil within a certain depth of the tension side was destroyed, and the damaged area was roughly fan-shaped on the surface. Furthermore, according to different failure forms, the calculation model under the oblique load and the fracture surface equation of the soil around the pile were established. Bhardwaj et al.[19] set up 10 different oblique angles to conduct uplift model experiments and analyzed the applicability of various existing theories to calculating tilt failure loads at different angles. Ramadan et al.[20,21] used centrifuge tests and numerical simulation software to study the uplift resistance of anchor piles in sand. The effects of factors such as the initial tension angle, bending moment, and solid pressure on the uplift resistance of anchor piles are discussed in depth. Aquaculture engineering is currently mainly used in coastal environments; however, a large amount of silty clay is deposited on the offshore seabed. Ramadan et al.[20,21] analyzed the uplift resistance capacity of anchor piles in sand but not in clay. The above literature review focuses on piles for construction engineering in which the structure size is much larger than the anchor piles used for marine aquaculture. Therefore, research must be conducted on the uplift resistance capacity of anchor piles according to their use in and the characteristics of the marine aquaculture environment.

This study investigates the uplift resistance capacity of the marine aquaculture anchor pile with different cases by means of a physical model experiment. Scientific selection and design of anchor piles can result in excellent safety performance of marine aquaculture equipment at a lower cost. A series of model tests was conducted with the main objective of investigating the effect of the initial tension angle, pile diameter, embedded depth, and pile configuration on the uplift resistance to provide a practical guide for the application of anchor piles in marine aquaculture.

Materials and Methods

Test system

The experiment was conducted at the Marine Engineering Hydrodynamics Laboratory of the National Engineering Research Center for Marine Aquaculture, China. The test system consisted of four parts as shown in Figure 2 (a): a counterforce frame, model tank, uplift system, and loading system. The counterforce frame was constructed of aluminum profiles (40 mm × 40 mm cross-sectional size), on which all the experimental devices used were installed. The model tank (700 mm × 700 mm × 700 mm, length × width × height) was made of glass, with a wall thickness of 15 mm, and was used for the soil fill. The distance from the center point of the model tank to the inner wall of the tank was 335 mm, which was greater than 10 times the maximum diameter of the anchor pile model of 30 mm, which satisfies the boundary effect[22,23]. A smooth glass wall helps to reduce the friction between the inner wall of the tank and soil. In addition, a fixed aluminum profile was set around the tank to ensure the overall stability of the model tank during the experiment. The uplift system consisted of two pulleys fixed on a steel plate and a double-stranded twine rope with a diameter of 2 mm. The steel plate was fixed 0.5 m above the tank. The position of pulley 1 can be moved, and pulley 2 was fixed directly above the loading system. The rope was connected to the anchor pile model and the loading system after passing through the two pulleys. The angle of the initial pulling force can be adjusted by changing the position of pulley 1. The load-ing system consisted of a loading box and weights.

During the experiment, as shown in Figure 2 (a), a tension sensor (Bengbu Dayang Sensor Co., Ltd., range: 0-100 N, accuracy: 0.3%) installed between pulley 1 and the anchor pile model was used to monitor the load in real time. A charge-coupled device (CCD) camera (Qingdao Optical Flow Software Technology Co., Ltd., size: 2560 × 2048 pixels) in-stalled on the outside of the model tank accurately captured the position information of the pile top of the anchor pile model under different tension loads without contact, as shown in Figure 2 (b), and then used to evaluate the uplift resistance capacity of the anchor pile model.

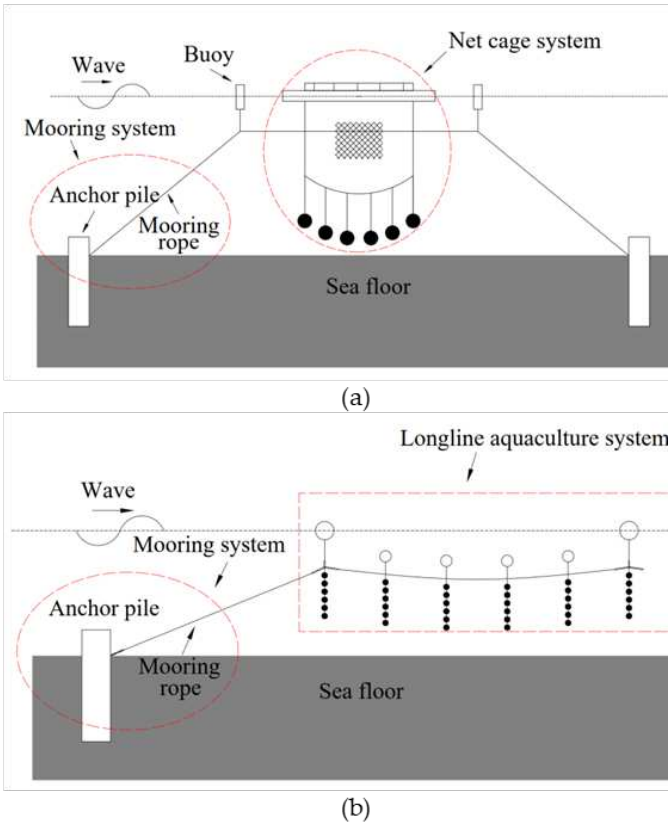

Figure 1. Schematic of common anchor piles used for aquaculture in marine facilities: (a) Net aquaculture system,(b) Longline aquaculture system.

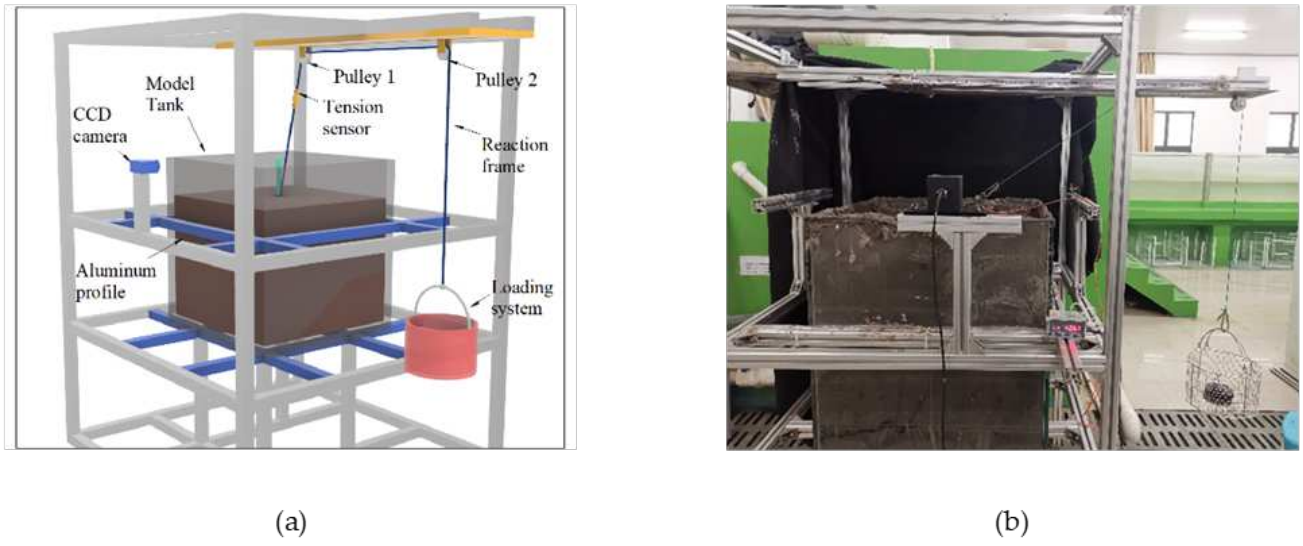

Figure 2. Diagrams of the test system: (a) Schematic of the test system; (b) Photograph of the test system.

Model anchor pile

In this experiment, the anchor pile model was mainly affected by oblique uplift force. When designing the anchor pile model, the geometric and force field similarity to real anchor piles are the main considerations[24]. The primary parameters of the prototype and model must satisfy the following relationships:

$$C_L = \frac{L_P}{L_M} \tag{1}$$

$$E_M I_M = \frac{1}{C_L^5} E_P I_P \tag{2}$$

where L_P, E_P , and I_P are the characteristic length, elastic modulus, and moment of inertia of the prototype, respectively, and L_M,E_M, and I_M are the characteristic length, elastic modulus, and moment of inertia of the model, respectively. Thus,C_L is a proportionality constant. The material of the prototype anchor pile was assumed to be steel, and the size parameters were pile diameter D = 140 mm, wall thickness t = 5 mm, and bending stiffness EI = 205 GPa. Based on the similarity theory, C_L = 1:7 was used as the scaling factor, and the model was made using 2 mm thick plexiglass. The flexural rigidity of the 20 mm diameter model anchor pile measured by a simple cantilever beam test was 136.2 Pa. Because the empirical calculation conformed to Equations 1 and 2, this study was based on this model, and the research was conducted by changing the size parameters. To simulate the friction between the anchor pile and the soil, the surface of the anchor pile model was sandblasted with quartz sand (180 mesh). The bottom of Figure 3 (a) shows the model of the anchor pile before sand blasting. Figure 3 (a–c) shows the different models used in the experiment. Different pile diameters (10, 20, and 30 mm), pile lengths (400, 500, and 600 mm), and pile configurations (circular single pipe, circular dual pile, square single pipe, square dual pile) were used. Hereinafter, anchor piles constructed of two pipes are referred to as the dual pile. According to aquaculture practices and previous research[20], fishermen bury the tension point of the anchor pile in the soil, but the depth of embedment varies from place to place, and there is no uniform standard. In this study, this difference is ignored, and the tension point of the anchor pile model is uniformly set on interface between the model and the soil of the soil, 6 cm from the top of the model, As shown in Figure 3 (d). In addition, to ensure that the CCD camera can accurately capture the position information of the anchor pile model, a black circular feature point was set on the top of the anchor pile model.

Soil

The marine soil used in the experiment was obtained from Changzhi Island, Zhejiang Province, China. Before starting the experiment, the soil was sieved to remove internal impurities. Water was added and stirring done to make it fully saturated. After the treatment was completed, the physical parameters were measured. The soil was classified as silty soil, and the specific parameters are presented in Table 1.

Table 1. Experimental soil parameters.

Density ρ/(g· cm^{-}3)	Proportion G_s	Void ratio e_0	Moisture content ω / (%)	Liquid limit ω_L / (%)	Plastic limit ω_P / (%)
1.67	2.73	1.555	56.3	40.2	22.5

Test step

To systematically study the uplift resistance capacity of anchor piles used in marine aquaculture, six test cases were designed as listed in Table 2. Here, D is the pile diameter, L is the embedded depth, and θ is the initial tension angle. Cases 1 and 2 were used to study the uplift resistance capacity of circular and square single piles, respectively, under different initial tension angles. Cases 3 and 4 were used to study the uplift resistance capacity of circular single piles with different pile diameters and embedded depths, respectively. Cases 5 and 6 were used to study the uplift resistance capacities of different pile configurations. The main experimental steps were as follows: 1. The processed soil was poured into the model tank and stirred continuously during the filling process to keep the soil even then left to stand for a week still after filling. 2. The anchor pile model was pressed into the soil slowly to avoid disturbing the soil around the model anchor pile during the pressing process. Once the pile was set, the test systems, such as the CCD cam-era and tension sensor, were powered. 3. The experiment adopted a fast maintenance load method. First, the load was gradually increased to record the position information of the top of the anchor pile under various loads. Second, after the displacement was stable, the next level of load was applied, and the experiment was stopped when the anchor pile failed. Each load was approximately 1/10 of the estimated failure load. 4. After the pile anchor fails, pull out the model and stirred the soil and leveled to start the next set of experiments.

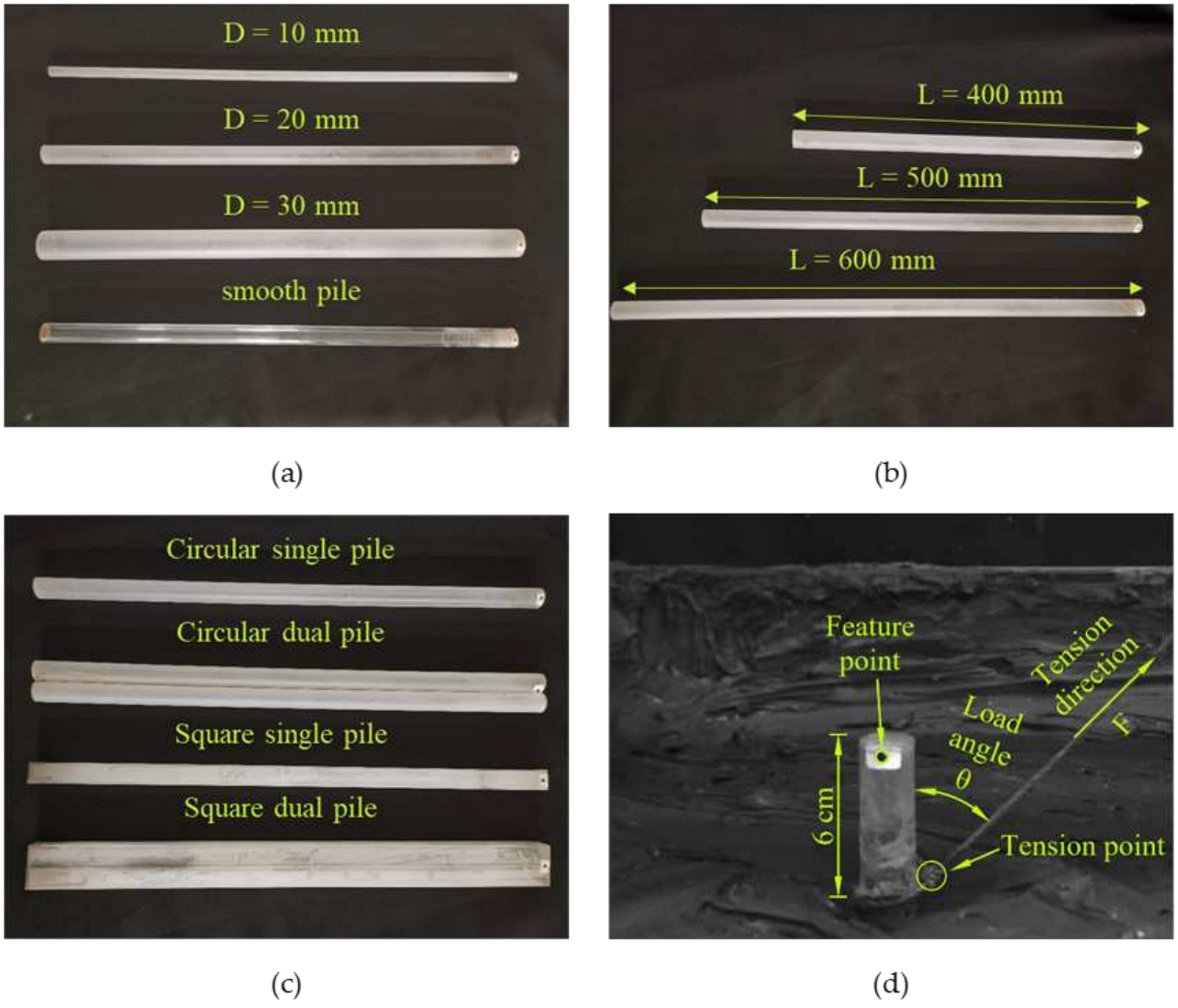

Figure 3. The model anchor piles used in the experiment and installation diagram: (a) Different pile diameter model; (b) Different pile length model; (c) Different pile configuration model; (d) Model anchor pile in test.

Table 2. Experimental soil parameters.

Case	Pile type	Diameter D/mm	Embedded depth L/mm	Initial tension angle θ/°	Dual pile layout angle /°
1	Circular single Pile	20	440	0,15,30,45,60	/
2	Square single pile	20	440	0,15,30,45,60	/
3	Circular single pile	10,20,30	440	30,45,60	/
4	Circular single pile	20	340,440,540	30,45,60	/
5	Circular dual pile	20 (single)	440 (single)	30,45,60	0,90
6	Square dual pile	20 (single)	440 (single)	30,45,60	0,90

Anchor pile failure standard

Under the oblique load condition, the displacement–load curve usually has not exhibit a distinct plunge point[25]. Therefore, the selection of the failure standard greatly affects the determination of the failure load of the anchor pile, and there is currently no failure load standard for marine aquaculture anchor piles. Yang et al.[18] suggested that the end loading standard of the oblique load test in cohesive soil is when the lateral dis-placement reaches 0.15 D. Qiu et al.[26] took the minimum value of the load corresponding to the maximum allowable displacement in different directions as the failure load. Bhardwaj et al.[19,25] summarized the determination methods for various failure loads in the uplift test and concluded that the double tangent method was more reasonable. In addition, Cortes-Garcia et al.[2] believe that the failure standards for onshore structures are too strict for offshore structures. Therefore, relatively loose failure standards should be formulated for the anchor piles used in marine aquaculture. Based on the above theory and combined with the experimental cases, the following anchor pile failure standards were defined. 1. Under the action of a single-stage load, the vertical or lateral displacement of the pile top increased suddenly, and the displacement–load curve had an obvious distinct plunge point. 2. The cumulative vertical displacement of the pile top is greater than 0.5 D. 3. The cumulative lateral displacement of the pile top was greater than 1 D.

Data processing

In this experiment, the tension action point of the model anchor pile was on the surface of the soil, and the displacement was relatively large and difficult to measure directly. Measuring the displacement of the feature point on the pile top indirectly reflects the position change of the model anchor pile during the tension process. In the experiment, a CCD camera was used to capture and record the position information of the anchor pile model, and the image was analyzed and processed to obtain the pile top displacement of the anchor pile model.

Results and discussion

Effect of initial tension angle on uplift resistance capacity

The initial tension angle is a key factor that must be considered during the installation of the anchor pile. This study (Cases 1 and 2) investigated the effect of the initial tension angle, set by moving pulley 1, on the uplift resistance capacity of the anchor pile (circular single pile and square single pile). To study the uplift capacity of anchor piles, this paper presents an analysis and detailed discussion on the magnitude and performance of failure loads, anchor pile displacements, and displacement development speeds.

Figure 4 shows the pile top displacement–load curves of the circular and square single piles under different initial tension angles. To obtain a better understanding of the uplift resistance capacity of the anchor pile, this study focuses on analyzing the data from the beginning of loading to the failure of the anchor pile. The endpoints of all displacement–load curves in this study are the corresponding loads and displacements at the moment of failure of the anchor pile. The load corresponding to the end of the curve is the failure load, and the displacement corresponding to the end is the maximum displacement before failure. The total displacement of the pile top during the experiment was analyzed in two directions, lateral and vertical. In this experiment, except for $\theta = 0°$ (θ is the initial angle of tension), the initial tension angle cases have lateral displacements. As shown in Figure 4, the initial tension angle has a significant effect on the top displacement of the circular and square single piles. For circular single piles, when the initial tension angle is small ($\theta = 0°$, 15°, 30°), as the load increases, the lateral and vertical displacements of the pile top slowly increase. The failure load was small, and both the lateral and vertical displacements were small. When the initial tension angle increased ($\theta = 45°$, 60°), as the load increased, the lateral displacement of the pile top developed rapidly, and the vertical displacement of the pile top developed slowly. The failure load and the maximum lateral and vertical displacements were all relatively large. For square single piles, when the initial tension angle is small ($\theta = 0°$, 15°, 30°), the lateral and vertical displacements and the total displacement were small. When the initial tension angle is large ($\theta =$ 45°, 60°), the displacement of the pile top, especially the lateral displacement, was large. Under the same initial tension angle cases, the square and circular single pile tops have similar dis-placement changes.

Figure 5 is a photograph of the failure process of the anchor pile model under $\theta = 60°$, where the left and right panels are for a circular square single pile, respectively. The yellow dotted line indicates the initial position of the marked feature point on the top of the anchor pile model, and F is the load on the anchor pile. As shown in Figure 5, as the load increased, the displacement of the square and circular single piles gradually increased, and the damage to the soil gradually became apparent. Table 3 summarizes the maximum displacements of the circular and square single piles under different initial tension angles, indicating that with an increase in the initial tension angle, the maximum lateral displacement and total maximum displacement of the model always increase, and the maximum vertical displacement initially increased and then decreased. Meanwhile, the maximum total displacement of the test cases of $\theta = 45°$ and $\theta = 60°$ was much larger than that of the other three groups of test cases. In addition, because the maximum total displacement was small when the initial tension angle was small ($\theta = 0°$, 15°, 30°), the deformation of the soil around the anchor pile was not apparent. However, when the initial tension angle was large (θ = 45°, 60°), the maximum total displacement and the deformation of the soil were large.

Figure 6 shows the anchor pile displacement and soil deformation before the failure of the circular single pile at $\theta = 60°$. Red area *I* is the soil deformation caused by the lateral displacement of the anchor pile. Yellow area *II* is due to insufficient cohesion be-tween the soil around the pile and the failure cracks caused by the deformation of the soil. The white area *III* is due to the accumulation of soil after deformation and the driving effect of the vertical displacement of the anchor pile, and the uplifting of the soil on the tension side. Because the seabed environment is complex, this form of soil destruction is not representative of deformation. However, the analysis and discussion of the deformation will help explain the mechanism of the interaction between the anchor pile and soil.

Reddy et al.[13] studied the uplift resistance capacity of piles under no lateral and lateral loading by applying a constant lateral load in an uplift model experiment. They found in the uplift test that when a constant load of 0.8 of the failure loads was applied in the transverse direction, the maximum total displacement of the pile top was 21 times the total displacement of the uplift load case ($\theta = 0°$). In this experiment, the maximum total displacement of the circular and square single pile under the $\theta = 60°$ test case was in-creased by factors of 20.9 and 15, respectively, compared with the maximum total dis-placement under the $\theta = 0°$ test case. Because Reddy et al.[13] used a circular pile as the experimental model, the maximum total displacement of the circular single pile in this experiment increased by a factor of 20.9, which is closer to the results in the literature. The maximum total displacement of the square single pile only increased by a factor of 15 owing to the difference in the anchor pile section, which differs from the results in the literature.

Table 3. Maximum displacement of pile top before failure on different initial tension angles.

Pile type	Maximumdisplacement	0°	15°	30°	45°	60°
Circular single pile	Lateral	/	1.11	4.13	17.78	19.21
	Lateral	0.95	2.06	3.65	7.30	5.08
	Total	0.95	2.34	5.51	19.22	19.87
Square single pile	Lateral	/	1.27	5.71	16.19	28.10
	Lateral	1.90	4.60	7.78	7.78	7.14
	Total	1.90	4.77	9.65	17.96	28.99

With an increase in the initial tension angle, the uplift resistance capacity of the anchor pile was significantly improved. The failure loads of a circular single pile under initial tension angles of 0°, 15°, 30°, 45°, and 60° were 9.80, 11.76, 16.17, 21.56, 24.50 N, respectively. Compared with the test case of $\theta = 0°$, the failure load increased by 20%, 65%, 120%, and 150%, respectively. The failure loads of a square single pile under initial ten-sion angles of 0°, 15°, 30°, 45°, and 60° were 13.72, 15.68, 19.60, 23.52, 26.95 N, respectively. Compared with the test case of $\theta = 0°$, the failure load increased by 14.3%, 42.9%, 71.4%, and 96.4%, respectively. In addition, the failure load of the square single pile under the same initial tension angle was larger than that of the circular single pile. This is because the cross-sectional area of a square with a side length of 20 mm is larger than that of a circular cross-sectional area of 20 mm. therefore the contact area between the square single pile and the soil was larger, the soil provided more reaction force, thereby increasing the failure load.

Kong et al.[27] believed that when $\theta > 0°$, a "P-Δ" coupling effect between the lateral load and the vertical load will occur, and the relationship between the two satisfies the elliptic equation:

$$\left(\frac{F\sin\theta}{F_h}\right)^2 + \left(\frac{F\cos\theta}{F_v}\right)^2 = 1 \tag{3}$$

where F is the resultant force acting on the structure; F_h and F_v are the lateral and vertical failure loads, respectively; and θ is the initial tension angle. It can be seen from equation 3 that the existence of a lateral load reduces the vertical uplift resistance. Rao et al.[6] and Gao et al.[28] determined, through laboratory model uplift tests of suction piles that the failure load of the suction pile was the largest when it was uplifted vertically ($\theta = 0°$). Fur-ther, the failure load gradually decreases with an increase in the initial tension angle, reaching the minimum when the lateral load is $\theta = 90°$. However, this theory fails to ex-plain fully the coupling between the lateral load and the vertical load. Conte et al.[14] concluded that the existence of lateral loads can improve the vertical uplift resistance ca-pacity of the structure[16,19].

Figure 7 shows the relationship between the lateral and vertical component forces of the anchor pile failure load and the initial tension angle. Figure 7 (a) and (b) represent cir-cular and square single piles, respectively. The figure shows that with the increase of the initial tension angle, the lateral component of the anchor pile failure load gradually in-creases, and the

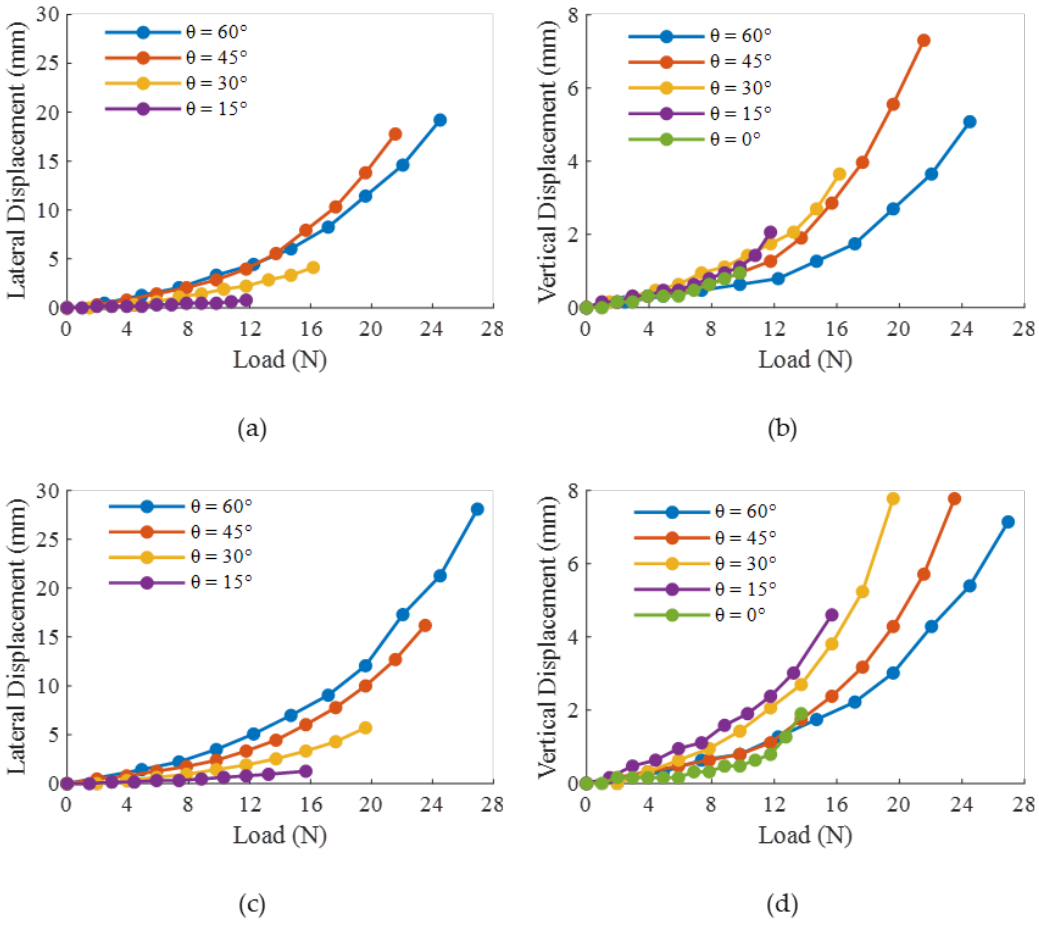

Figure 4. Displacement–load curve of anchor piles with different initial tension angles: (a) The lateral displacement–load curve of the circular pile; (b) The vertical displacement–load curve of the circular pile; (c) The lateral displacement–load curve of the square pile; (d) The vertical displacement–load of the square pile.

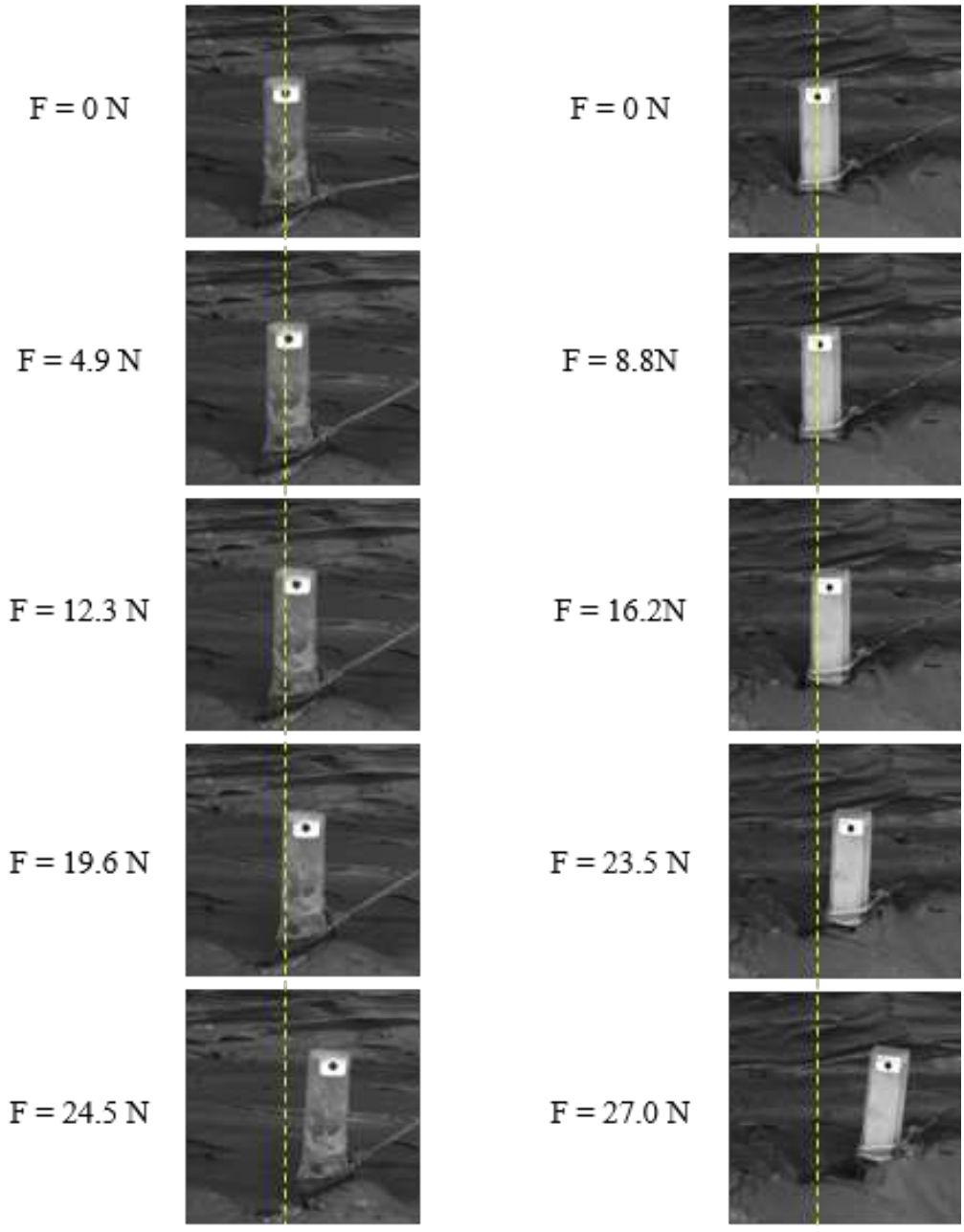

Figure 5. Photographs of the failure process of the anchor pile model. (The yellow dotted line indicates the initial position of anchor pile model. Left panel: circular single pile, $\theta = 60°$; right panel: square single pile, $\theta = 60°$).

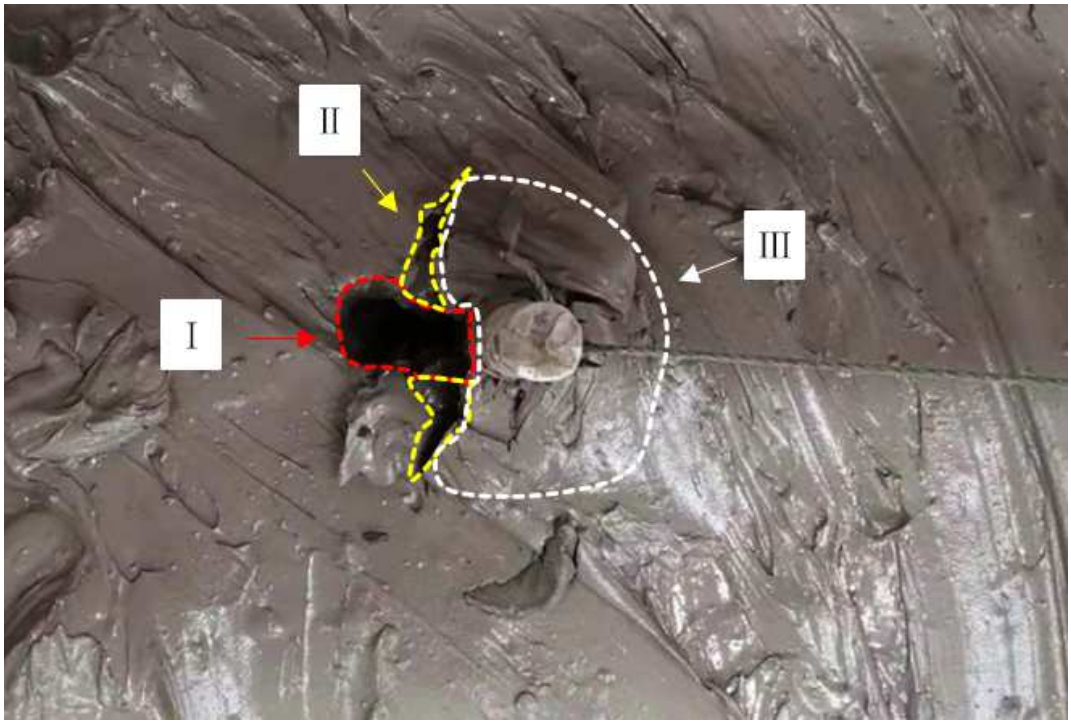

Figure 6. Photograph of the anchor pile displacement and soil deformation before failure (test case: circular single pile, θ = 60°).

vertical component initially increases and then decreases. This shows that the existence of the lateral force component in this experiment improves the vertical uplift resistance capacity of the anchor pile, thereby increasing the failure load of the an-chor pile, which conforms to the theory proposed by Conte et al. In this section of experi-ments, the vertical component of the failure load under the θ = 60° test case has decreased compared to the θ = 45° test case. Wen et al.[29] concluded that with the increase of the loading angle, the bearing mode of the pile gradually changed from mainly the vertical to the lateral bearing, and the lateral displacement of the pile top increased significantly. In this experiment, this phenomenon is also due to the change in the force form of the anchor pile, which caused excessive lateral displacement of the anchor pile, destroyed the soil around the anchor pile prematurely, and the vertical resistance was not fully exerted. Ta-ble 3 shows that the maximum vertical displacements of the two tube types under θ = 60° are smaller than those under θ = 45°, which also shows that premature failure of the an-chor pile occurs under θ = 60°.

In summary, increasing the initial tension angle improves the uplift resistance ca-pacity of the anchor pile but, simultaneously, causes a larger displacement of the anchor pile. Generally, a large lateral displacement of structures is not allowed in marine engi-neering. However, considering the experimental results described in this section and ma-terial costs if the anchor pile has a good uplift resistance capacity, larger displacements should be allowed.

Effect of pile diameter on uplift resistance capacity

The effect of the pile diameter on the uplift resistance capacity of a circular single pile is shown in Figure 8. The figure shows the displacement–load curves of circular single piles with different pile diameters (D = 10, 20, and 30 mm and the specific model shown in Figure 2 (a)) at the initial tension angles of 30°, 45°, and 60° (Case 3). The left and right sides are the lateral and vertical displacement–load curves of the pile top. As shown in the figure, as the pile diameter increased, the slope of the lateral and vertical displacement–load curve of the pile top gradually decreased, and the curve becomes smoother. This shows that increasing the pile diameter effectively improved the uplift resistance capacity of the anchor pile. The lateral displacement–load curve on the left shows that when the anchor piles with different pile diameters (D = 10, 20, and 30 mm) were at θ = 30°, the cor-responding maximum lateral displacements were 4.76, 4.12, and 3.97 mm, respectively. When θ = 45°, the corresponding maximum lateral displacements are 11.90, 17.78, and 13.49 mm, respectively. When θ = 60°, the corresponding maximum lateral displacements are 20.48, 19.21, and 18.25 mm, respectively. There was no significant difference in the maximum lateral displacement for different pile diameters at the same tension angle. The vertical displacement–load curves on the right show that when the anchor piles with different pile diameters (D = 10, 20, and 30 mm) are at θ = 30°, the corresponding maximum vertical displacements are 2.38, 3.65, and 3.97 mm, respectively. When θ = 45°, the corresponding

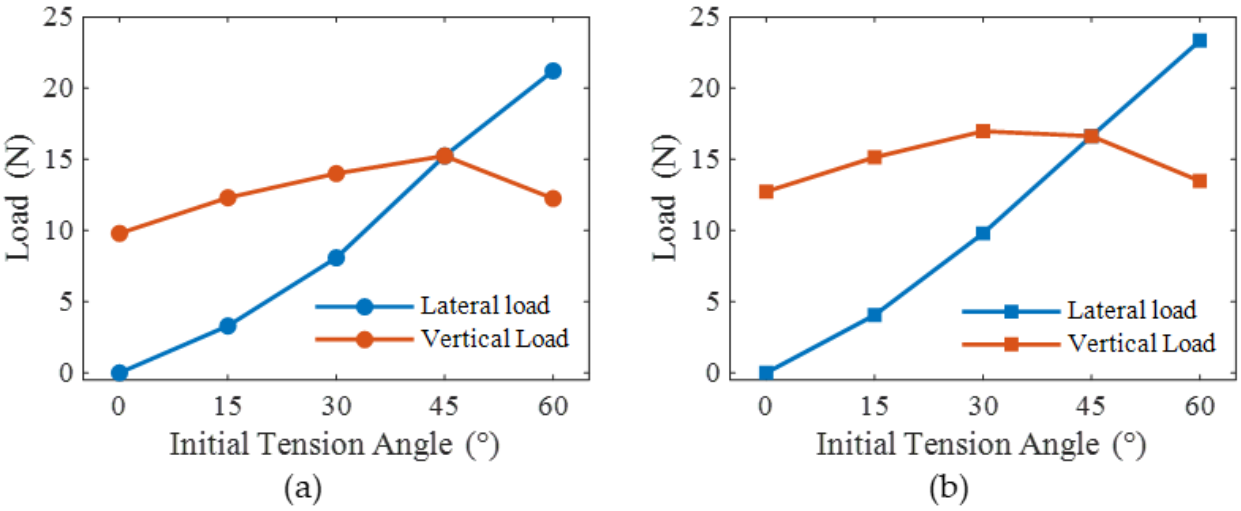

Figure 7. Relationship between the lateral and vertical component forces of anchor pile failure load with the initial tension angle. (a) Circular single pile; (b) Square single pile.

maximum vertical displacements are 3.17, 7.30, and 6.67 mm, respectively. When θ = 60°, the corresponding maximum vertical displacements are 1.75, 5.08, and 6.67 mm, respectively. The maximum vertical displacement for the D = 10 mm test case is significantly smaller than for the D = 20 and 30 mm test cases, and the maximum vertical displacements of the D = 20 and 30 mm test cases were not significantly different. In summary, the increase in pile diameter can effectively delay the development speed of displacement but has little effect on the maximum displacement. In addition, the tension angle is still the main factor affecting the displacement of the pile top, especially the lateral displacement.

Figure 9 shows a comparison of the failure loads of the anchor piles for different pile diameters. The failure load of the anchor piles increased as the pile diameter increased. Al-Mhaidib et al.[30] conducted an uplift test on three circular piles with different pile diameters (D = 45, 89, and 178 mm) and found that increasing the pile diameter can effectively improve the uplift resistance capacity of the pile. When θ = 30°, 45°, and 60°, the failure loads of the D = 10 mm test case were 5.88, 7.84, and 8.82 N, respectively. The failure loads of the D = 20 mm test case were 16.17, 21.56, and 24.5 N, and compared to those of the 10 mm pile diameters, the failure loads increased by 175.0%, 175.0%, and 177.8%, respectively. The failure loads of D = 30 mm were 23.52, 30.87, and 35.28 N, respectively, which are 45.4%, 43.2%, and 44% higher than those of D = 20 mm. Wang et al.[31] concluded that as the pile diameter increases, when the pile fails, the soil will change from a shallow wedge failure to a combination of shallow wedge failure and deep rotating soil flow; therefore, the anchor pile uplift resistance capacity will not increase with the in-crease in pile diameter by an equal margin. Although the number of pile diameter sam-ples in this experiment was not sufficient, the improvement in the failure load of D = 30 mm compared to D = 20 mm was significantly smaller than that of D = 20 mm compared to D = 10 mm. In addition, the figure shows that the failure load gradually increases with an increase in the initial tension angle. When θ = 45°, the failure loads of the three pile diameters (D = 10, 20, and 30 mm) of the anchor piles increased by 33.3%, 33.3%, and 31.3%, respectively, compared with θ = 30°. When θ = 60°, the failure loads of the three pile diameters (D = 10, 20, and 30 mm) increased by 50%, 51.5%, and 50%, respectively, com-pared with θ = 30°. This shows that increasing the pile diameter does not change the effect of the initial tension angle on the uplift resistance capacity. Rahman et al.[32] conducted laboratory model uplift experiments and found that the initial tension angle has the same effect on the uplift resistance capacity of expanded-bottom piles with different diameters. Sharma et al.[33] studied the uplift resistance capacity of axial granular anchor piles in-stalled obliquely and found that as the pile diameter increased, the uplift resistance capacity of the encased axial granular anchor pile significantly improved and was not affected by the installation inclination angle.

Effect of embedded depth on uplift resistance capacity

The effect of the embedded depth on the uplift resistance capacity of a circular single pile is shown in Figure 10. The figure shows the displacement–load curves of the pile anchors with different embedded depths (L = 340, 440, and 540 mm; and the specific model shown in Figure 2 (b)) at 30°, 45°, and 60° initial tension angles (Case 4). The left and right panels are for the lateral and vertical displacement–load curves of the pile top. The figure shows that for the three initial tension angles, the displacement–load curves of different embedded depths differ significantly. From the lateral displacement curves on the

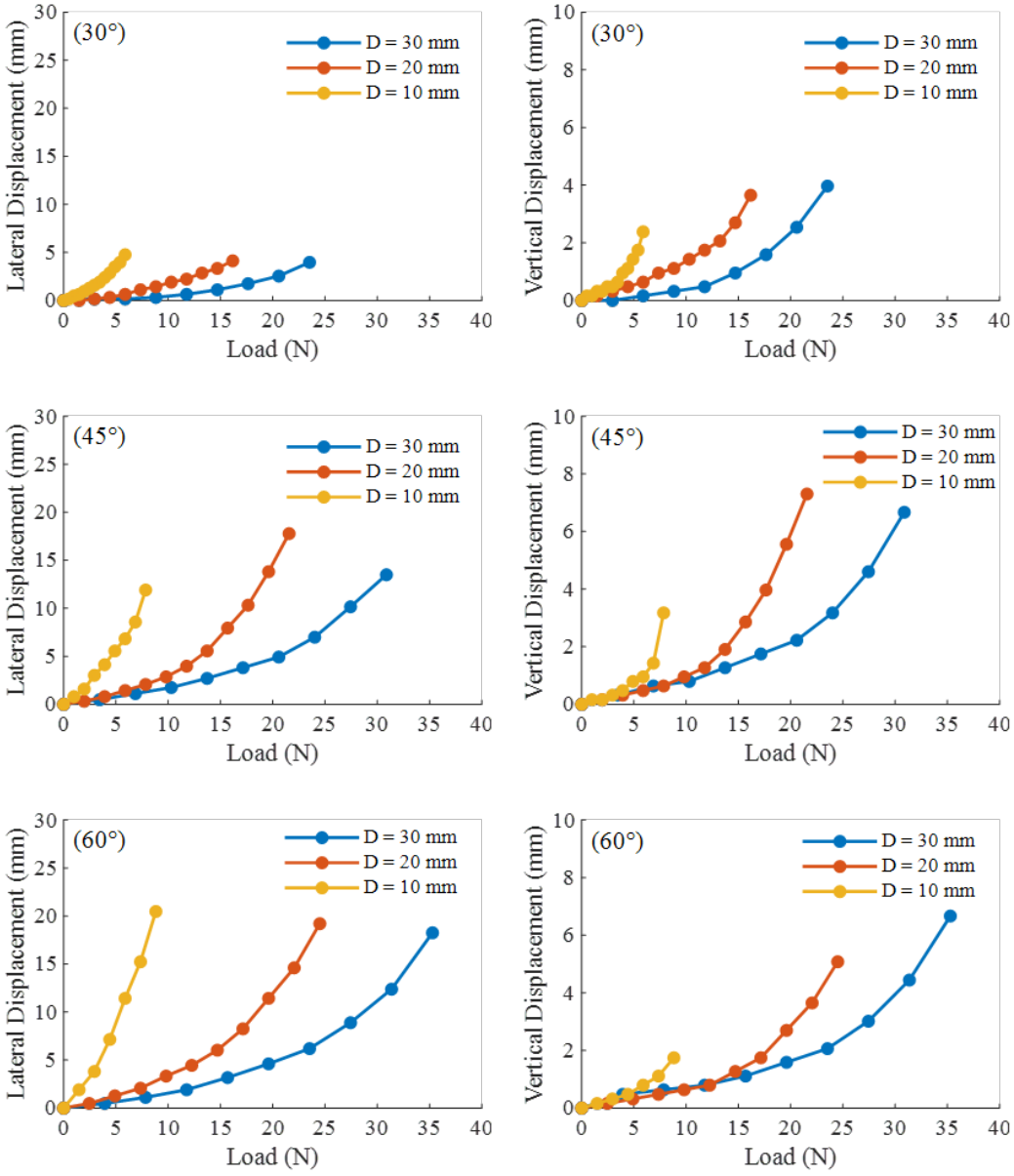

Figure 8. Displacement–load curve of a circular single pile for different pile diameters (left panel: lateral displacement–load curve, right panel: vertical displacement–load curve).

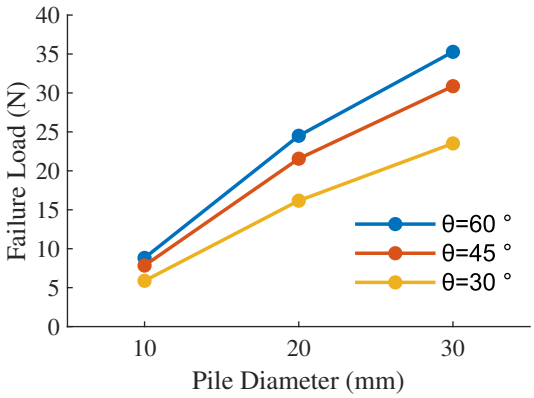

Figure 9. Figure 9. Failure loads of anchor pile models with different pile diameters.

left, the curve for L = 340 mm developed the fastest among the three cases. For small loads, the curves of L = 440 mm and L = 540 mm have similar slopes, and the curves partially over-lap. As the load increased, the anchor piles for L = 440 mm fail, and the displacement in-creased rapidly. The curves of L = 440 mm and L = 540 mm appear to be different. From the vertical displacement–load curve on the right, the curve slopes gradually decrease with an increase in the embedded depth. The displacement development speed of the L = 540 mm test case was the slowest. Increasing the embedded depth effectively delayed the development speed of vertical displacement.

Figure 10 shows that when θ = 30° for different embedded depths (L = 340, 440, and 540 mm), the corresponding maximum lateral displacements were 1.27, 4.12, and 6.98 mm, respectively. When θ = 45°, the corresponding maximum lateral displacements were 10.00, 17.78, and 24.44 mm, respectively. When θ = 60°, the corresponding maximum lateral displacements were 20.15, 19.20, and 33.65 mm, respectively. Ai et al.[34] used finite element analysis to study the force characteristics of piles with different embedded depths under lateral loads and found that increasing the embedded depth could not effectively limit the development of lateral displacement. In this experiment, except for the L = 340 mm case when θ = 60°, the maximum lateral displacement may be slightly larger than the L = 440 mm case because of experimental errors. In other cases, the maximum lateral dis-placement of the pile top increased with the embedded depth. L = 540 mm was the largest among the three embedded depths. For different embedded depths (L = 340, 440, and 540 mm) at θ = 30°, the corresponding maximum vertical displacements were 1.26, 3.65, and 2.54 mm, respectively. When θ = 45°, the corresponding maximum vertical displacements were 5.71, 7.30, and 3.96 mm, respectively. When θ = 60°, the corresponding maximum vertical displacements were 4.92, 5.07, and 2.69 mm, respectively. Thus, the maximum vertical displacement for L = 440 mm is the largest among the three embedded depths, and the maximum vertical displacement for L = 540 mm is the smallest.

Figure 11 shows the relationship between the anchor pile failure load and the em-bedded depth under different initial tension angles. The figure shows that the failure load increased with an increase in embedded depth. When θ = 30°, 45°, and 60°, the failure loads of L = 340 mm were 6.86, 11.76, and 15.68 N, respectively. The failure loads of L = 440 mm were 16.17, 21.56, and 24.50 N, respectively, and compared with L = 340 mm, in-creased by 135.7%, 83.3%, and 56.3%, respectively. The failure loads of L = 540 mm were 26.46, 39.2, and 35.28 N, respectively, and compared with L = 440 mm, increased by 63.6%, 81.8%, and 44%, respectively. Gaaver et al.[35] found two main explanations for why the embedded depth improves the uplift resistance. 1. Improved friction in the pile–soil inter-face. Thus, the increased embedded depth increase the effective stress in the anchor pile and the soil shear strength. 2. Increased contact area between the anchor pile and soil. Emirler et al.[36] used numerical simulations to study the uplift resistance capacity of piles with different embedded depths in sand and found that the area of effect of the anchor pile on the soil surface increased with an increase in the embedded depth. Although in this study, the effect of the anchor pile under oblique load differs slightly from the above research, increasing the embedded depth still increases the uplift resistance capacity of the anchor pile.

When θ = 45°, the failure loads of the different embedded depths (L = 340, 440, and 540 mm) of the anchor piles increased by 71.4%, 33.3%, and 48.1%, respectively, compared with θ = 30°. When θ = 60°, the failure loads of the different embedded depth depths (L = 340, 440, and 540 mm) of the anchor piles increased by 128.6%, 51.5%, and 33.3%, respectively, compared with θ = 30°. For L = 340 mm and L = 440 mm, the failure load of the an-chor pile increased as the initial tension angle increased. In the L = 540 mm case, the failure load of the θ = 45° test case was greater than that of the θ = 60° and θ = 30° cases, which shows that the uplift resistance capacity no longer increased with an increase in the initial tension angle. Jamnejad et al.[37] conducted experimental and theoretical studies on anchor piles installed vertically in saturated non-cohesive soil and concluded that the uplift resistance capacity of anchor piles under oblique loads would increase with embedded depth.

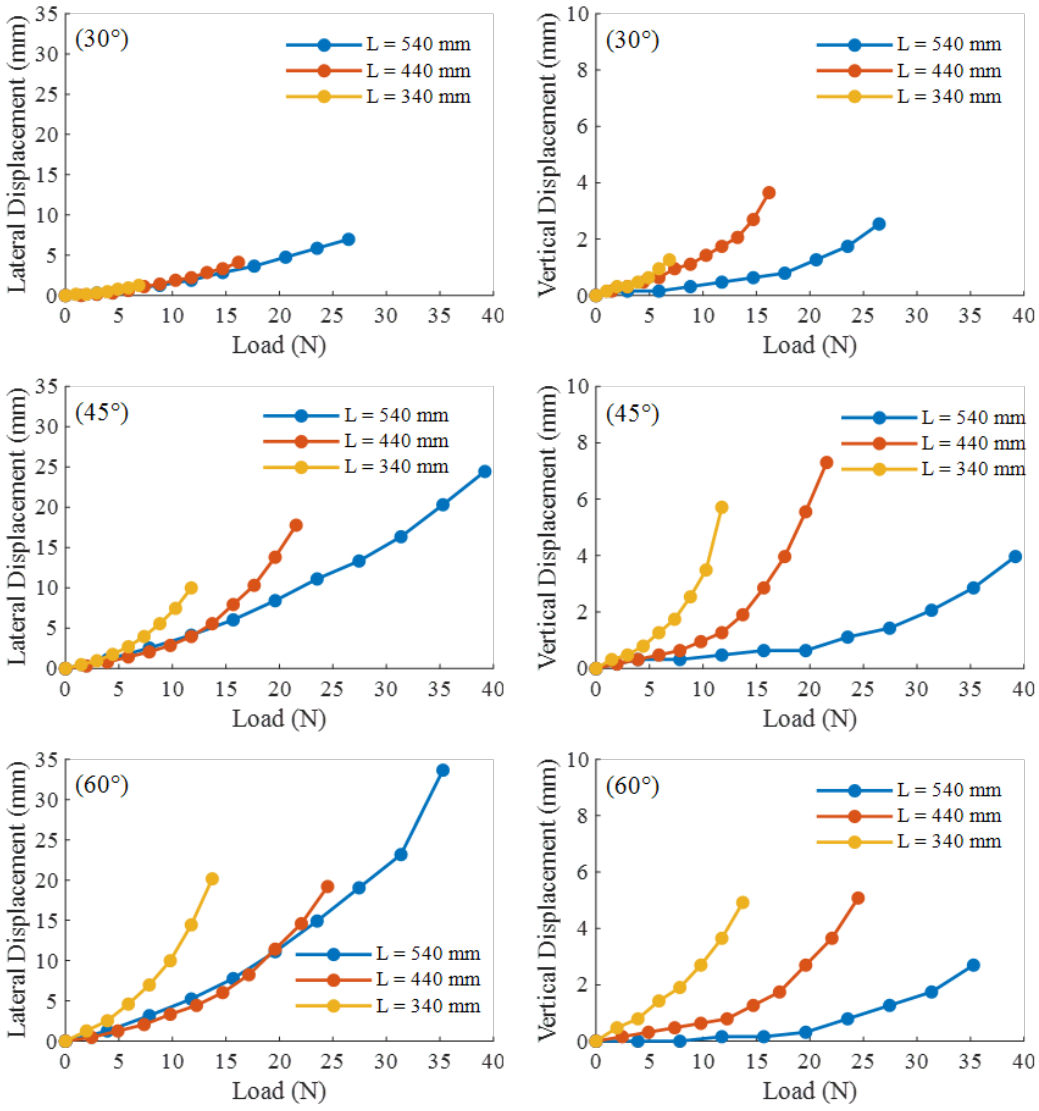

Figure 10. Displacement–load curve of circular anchor piles under different embedded depths (left panel: lateral displacement–load curve, right panel: vertical displacement–load curve).

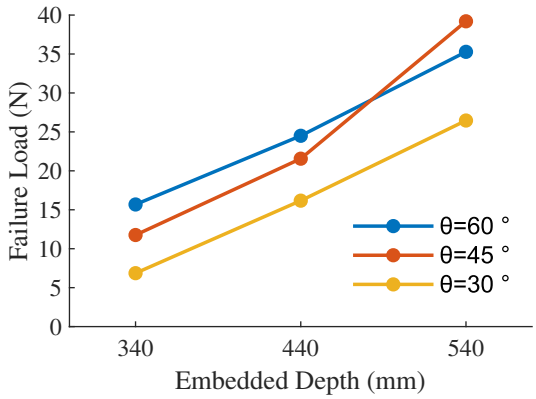

Figure 11. Anchor pile failure load under different embedded depths.

When the embedded depth reaches a certain level, a further increase in the embedded depth can only lead to an increase in the vertical component, and the effect on the lateral component and the improvement in the uplift resistance capacity are no longer significant. In this experiment, the reason for the decrease in the failure load at $\theta = 60°$ may be that the lateral soil reaction force increased as the embedded depth increased, the soil could not provide sufficient reaction force, and the anchor pile failed prematurely.

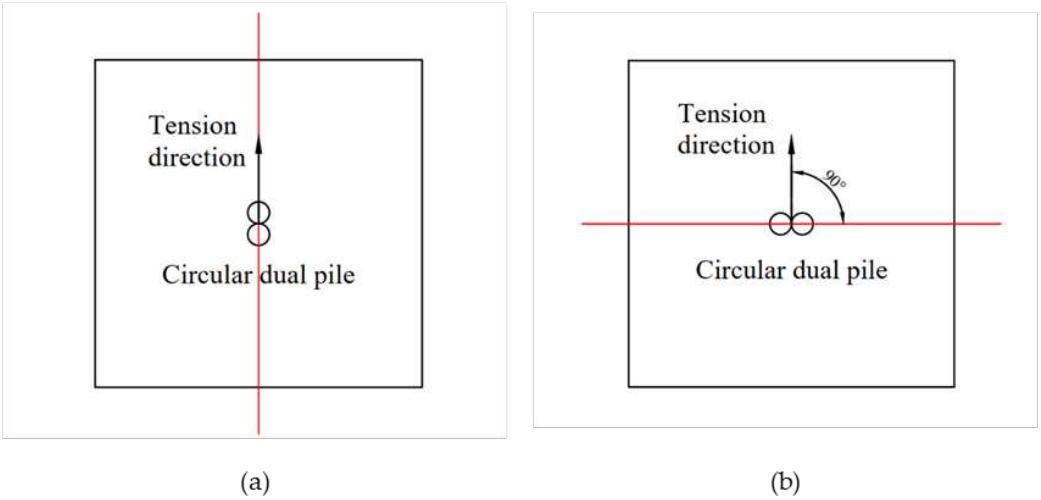

Figure 12. Schematic of the different dual pile model layouts. (a) 0°_dual layout; (b) 90°_dual layout.

Effect of pile configuration on uplift resistance capacity

In marine aquaculture, two anchor piles are often tied together to improve the uplift resistance capacity of the anchor piles. In this section, two-pipe anchor pile models were posted side-by-side using plexiglass glue to simulate a two-pipe anchor pile. The dual anchor pile model used in this experiment is shown in Figure 2 (c). To study the effect of pile configuration on the resistance to uplift resistance capacity, dual piles are installed using two methods. Figure 12 illustrates the specific situation. 0° and 90° represent the angle between the dual pile model and the tension direction.

Figures 13 and 14 show the displacement–load curves for different pile configurations of circular and square anchor piles (single pile, 0°_dual layout, 90°_dual layout) under the initial tension angles of 30°, 45°, and 60° (Cases 5 and 6). The figures show that the development speed of the lateral and vertical displacements of the dual pile was significantly lower than that of the single pile. Table 4 shows the maximum displacements for different pile configurations. From Figure 13 and Table 4, when $\theta = 30°$, the lateral dis-placement–load curves of the 0°_dual layout and 90°_dual layout have similar slopes and high curve coincidence. The vertical displacement–load curve of the 90°_dual layout was slightly faster than that of the 0°_dual layout. From the perspective of maximum dis-placement, the lateral and vertical displacement of the 90°_dual layout were larger. When $\theta = 45°$, the lateral and vertical displacement–load curves of the two layouts also have a certain coincidence,

but the difference between the curves was larger than for $\theta = 30°$, and the maximum displacement difference between the horizontal and vertical directions was smaller. When $\theta = 60°$, there were clear differences in the displacement development of the two layouts. The lateral displacement–load curve of the 90°_dual layout and the corresponding 0°_dual layout develops slowly. Therefore, the lateral displacement of the 0°_dual layout was greater than that of the 90°_dual layout, and the vertical displacement of the 90°_dual layout was greater than that of the 0°_dual layout. As shown in Figure 14 and Table 4, the displacement development and maximum displacement of the square anchor piles under different pile configurations were similar to those of the circular anchor piles.

Figure 15 demonstrates the differences in pile configurations more intuitively. It shows photographs of the destruction process of different pile configurations. The figure shows that the load required for the same displacement of the circular single pile was less than that of the dual pile. When the applied load F was the same, the displacement of the circular 90°_dual layout was smaller than that of the 0°_dual layout. This shows that although the cross-sectional area of the 90°_dual layout in the tension direction was twice that of the 0°_dual layout, in this experiment, only the 90°_dual layout effectively reduced the development of lateral displacement when $\theta = 60°$. Thus, when the initial tension angle is small, the lateral soil reaction force required by the dual pile is small, and the full effect of the increased cross-sectional area is not realized. In marine aquaculture, a 90°_dual layout should be used when a large lateral force component is required.

Table 4. Maximum displacement of pile top before failure at different initial tension angles.

Layout angle	Initial tension angle	Circular dual pile			Square dual pile		
		Lateral displacement	Vertical displacement	Failure load	Lateral displacement	Vertical displacement	Failure load
0°	30°	5.56	7.78	26.46	7.3	8.25	32.34
	45°	19.37	6.83	37.73	20.95	6.98	39.2
	60°	40	7.14	39.2	26.98	3.97	35.28
90	30°	6.67	6.98	29.4	7.62	5.71	35.28
	45°	16.67	7.78	39.2	20.16	7.46	43.12
	60°	25.4	10.32	39.2	20.95	5.56	39.2

The failure loads of the circular anchor piles with different pile configurations at $\theta = 30°$ were 16.17, 24.46, and 29.40 N. When $\theta = 45°$, the failure loads were 21.56, 37.73, and 39.20 N, respectively. When $\theta = 60°$, the failure loads are 24.50,39.20, and 39.20 N, respectively. The failure loads of different pile configurations of square anchor piles at $\theta = 30°$ were 19.60, 32.34, and 35.28 N, respectively. When $\theta = 45°$, the failure loads were 23.52, 39.20, and 43.12 N, respectively. When $\theta = 60°$, the failure loads were 26.95, 35.28, and 39.20 N, respectively. Thus, the uplift resistance capacity of the dual pile was significantly better than that of the single pile. The uplift resistance capacity of the 90°_dual layout was better than that of the 0°_dual layout. Figure 16 shows the relationship between the failure load of the double-pipe anchor pile and the initial tension angle. The figure shows that when $\theta = 60°$ the failure load of the circular 0°_dual layout was the largest but only slightly larger than the failure load of $\theta = 45°$. In the circular 0°_dual layout, the failure loads at $\theta = 60°$ and $\theta = 45°$ were equal. The square 0°_dual layout $\theta = 45°$ failure load was the largest and was clearly greater than the cases of $\theta = 30°$ and $\theta = 60°$. For the square 90°_dual layout, the failure loads at $\theta = 60°$ and $\theta = 45°$ were equal. Regarding this phenomenon, Reddy et al.[13] concluded that when the oblique tension load was too large, the lateral reaction force of the soil around the anchor pile was insufficient, and the anchor pile was destroyed prematurely, resulting in a reduction in the failure load. This could be the reason for the decrease in the failure load of the square dual pile at $\theta = 60°$ in this experiment. In addition, in the experiment discussed in last section on the effect of the em-bedded depth on the uplift resistance capacity, the embedded depth of 540 mm coincides with the maximum failure load in the case of $\theta = 45°$. This shows that in marine aquaculture, the best initial tension angle of anchor piles is not as large as possible, and factors such as soil quality and tube type should be comprehensively considered.

Conclusions

In this study, by performing oblique anchor pile uplift experiments on models, the effects of factors such as initial tension angle, pile type, pile diameter, embedded depth, and pile configuration on the uplift resistance capacity of anchor piles were

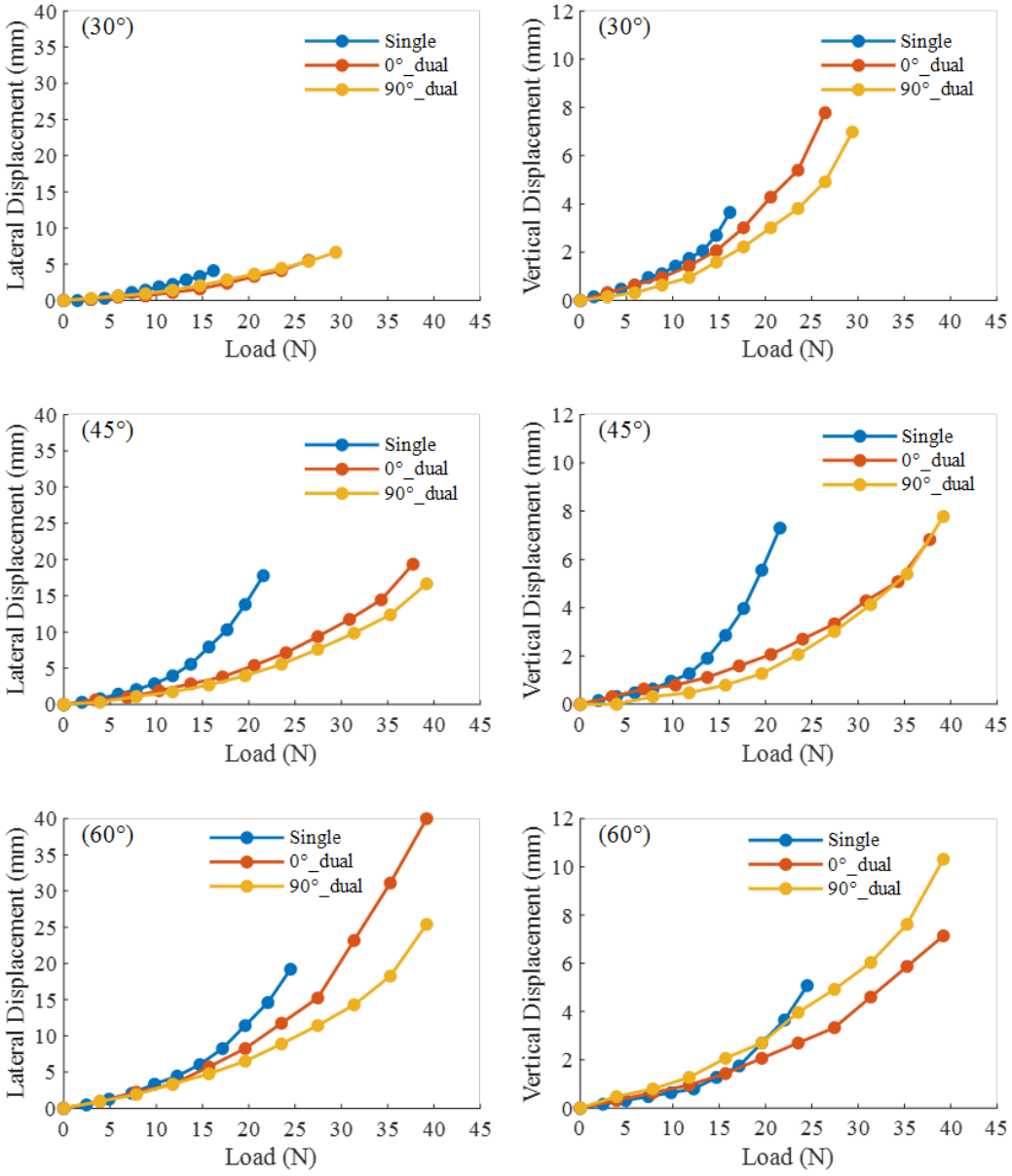

Figure 13. Displacement–load curve of different tubular circular anchor piles (left panel: lateral displacement–load curve, right panel: vertical displacement–load curve).

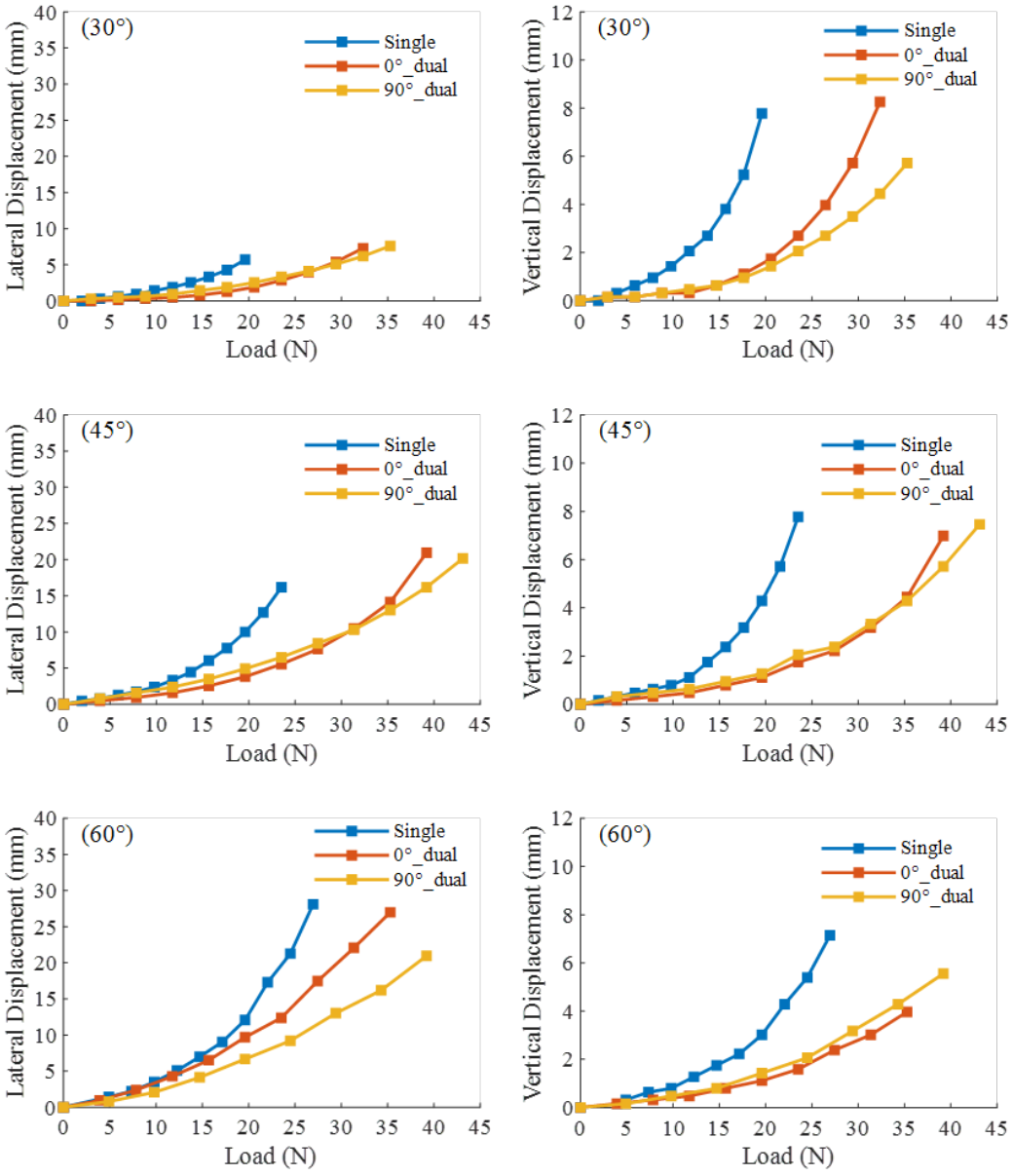

Figure 14. Displacement–load curve of different tubular square anchor piles (left panel: lateral displacement–load curve, right panel: vertical displacement–load curve).

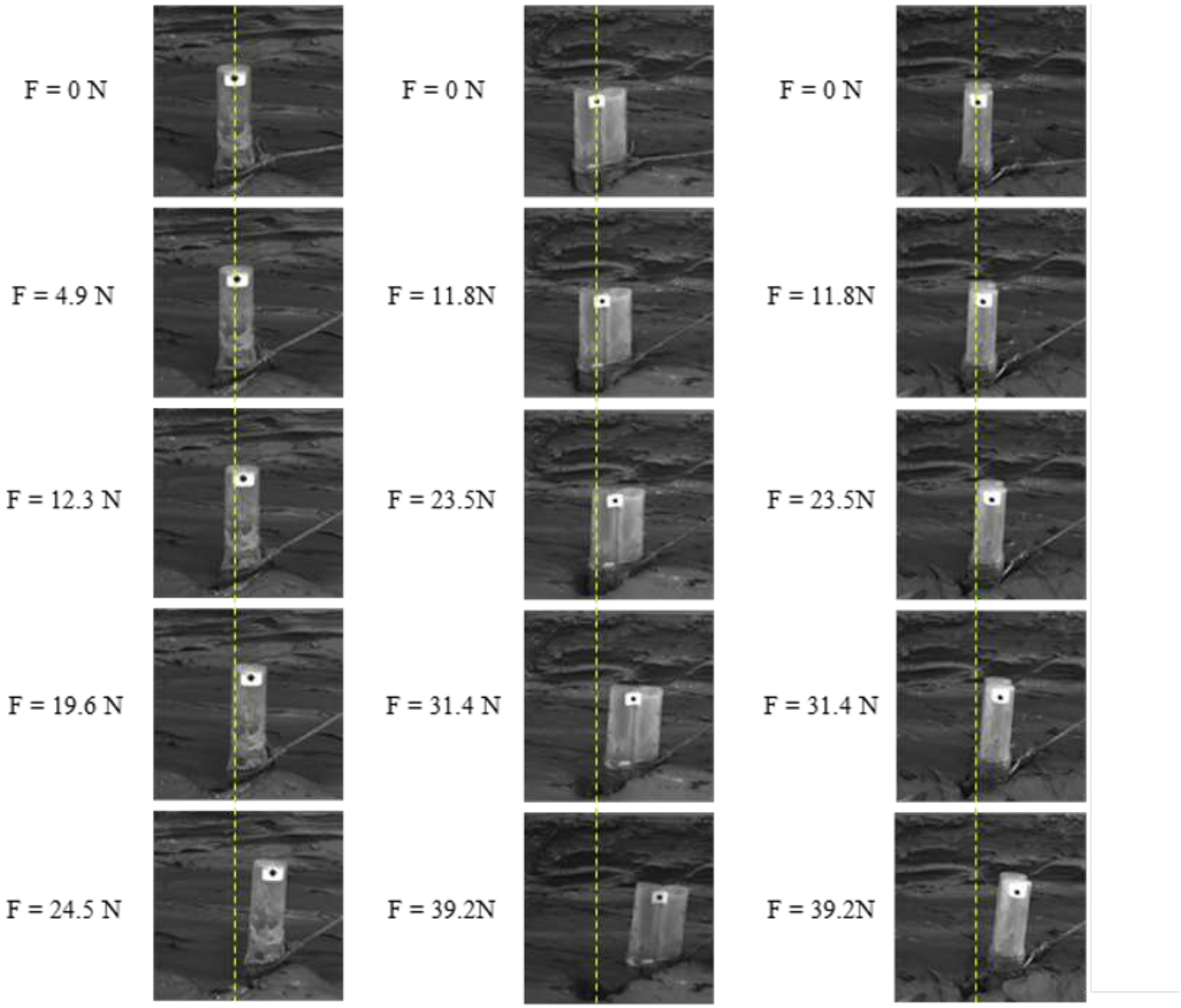

Figure 15. Photos of the destruction process of different pile configurations (the first panel shows circular single piles, θ = 60°; second panel shows the 0°_dual layout, θ = 60°; third panel shows the 0°_dual layout, θ = 60°; and yellow dotted line in-dicates the initial position of the model of anchor pile).

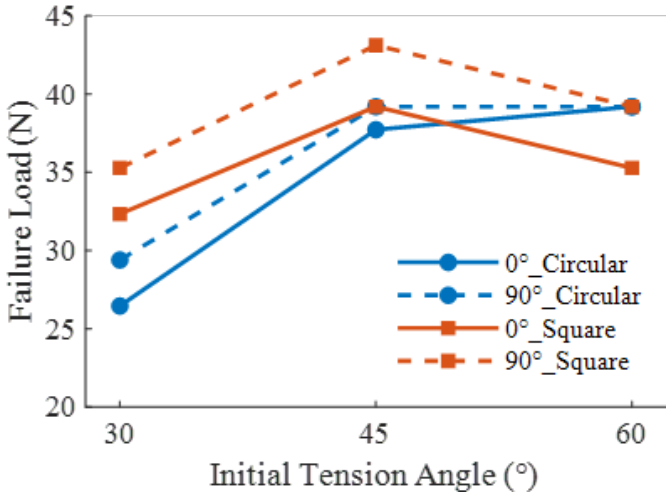

Figure 16. Relationship between the failure load of dual anchor pile and the initial tension angle.

determined, with the following conclusions:

- a circular and square single pile, both the uplift resistance capacity and the anchor pile top displacement development speed increased with an increase in the initial tension angle. When the initial tension angle was greater than 45°, the large lateral displacement drastically increased. Considering the limited cost for marine aquaculture, good tensile resistance maintained by the anchor pile should allow large displacement movement.

- Under the same initial tension angle, owing to the larger contact area of the square single pile with the soil, its uplift resistance capacity was slightly better than that of the circular single pile.

- An increase in the pile diameter can effectively improve the uplift resistance capacity of the circular anchor pile and delay the development speed of the pile top displacement. In-creasing the initial tension angle with the same pile diameter improves the uplift resistance capacity.

- The increase in the embedded depth can effectively improve the uplift resistance capacity of the circular anchor pile and increase the maximum lateral displacement of the pile top before failure. In the test case of $\theta = 45°$, the maximum failure load of the anchor pile occurred when L = 540 mm.

- The uplift resistance capacity of the dual pile was significantly better than that of the single pile. The uplift resistance capacity of the 90°_dual layout was slightly better than that of the 0°_dual layout, but the improvement was not significant. There was no clear difference in the displacement development of the two layouts in the $\theta = 30°$ and $\theta = 45°$ test cases. When $\theta = 60°$, the lateral displacement development of the 90°_dual layout was significantly smaller than that of the 0°_dual layout, and the vertical displacement of the 0°_dual layout was slightly larger than that of the 90°_dual layout. Changing the layout mode reduced the maximum lateral displacement only when the initial tension angle was large.

- In this study, in most test cases the larger the initial tension angle, the stronger the uplift resistance capacity; however, the circular dual pile in the $\theta = 60°$ test case had the largest failure load, which was only slightly larger or equal to that of the $\theta = 45°$ test case. The failure load of the square dual pile was the largest at $\theta = 45°$ and was greater than that at $\theta = 60°$. Further, the failure load when L = 540 mm was also the largest when $\theta = 45°$. There-fore, the initial tension angle should not be as large as possible, and a variety of factors should be considered when determining the design of the marine aquaculture facility.

Acknowledgements

The work was funded by the National Key Research and Development Program of China (Grant No. 2020YFE0200100), the National Natural Science Foundation of China (Grant No. 32002441,42076213). These financial supports are gratefully acknowledged.

Author contributions statement

Conceptualization, F.G., and X.Q.; methodology, F.G., and J.K.; validation, J.K., Y.Y., and F.Z.; formal analysis, J.K.; investigation, D.F., X.Q.; resources, J.K.; data curation, D.F.; writing—original draft preparation, J.K.; writing—review and editing, D.F.; visualization, D.F.; supervision, F.G. D.F.; project administration, F.G.; funding acquisition, F.G. X.Q. All authors have read and agreed to the published version of the manuscript.

Additional information

Competing interests The authors declare no conflict of interest. **Accession codes** Not applicable.

The corresponding author is responsible for submitting a competing interests statement on behalf of all authors of the paper. This statement must be included in the submitted article file.

References

1. *China Fishery Statistical Yearbook. 2019* (China Fisheries Bureau of the Ministry of Agriculture, 2019).
2. Cortes-Garcia, L. D., Landon, M. E., Gallant, A. P. & Huguenard, K. D. Assessment of helical anchor capacity in marine clays for aquaculture applications. In *Geo-Congress 2019: Foundations*, 299–307 (American Society of Civil Engineers Reston, VA, 2019).
3. Trujillo, E., León, L. & Martínez, G. Deadweight anchoring behavior for aquaculture longline. *Lat. american journal aquatic research* **48**, 686–695 (2020).
4. Hou, H.-M., Dong, G.-H., Xu, T.-J., Zhao, Y.-P. & Bi, C.-W. Dynamic analysis of embedded chains in mooring line for fish cage system. *Pol. Marit. Res.* (2018).
5. Gaudin, C. *et al.* Recent advances in anchor design for floating structures. *Int. J. Offshore Polar Eng.* **27**, 44–53 (2017).
6. Rao, S. N., Latha, K. H., Pallavi, B. & Surendran, S. Studies on pullout capacity of anchors in marine clays for mooring systems. *Appl. Ocean. Res.* **28**, 103–111 (2006).
7. Esfeh, P. K. & Kaynia, A. M. Numerical modeling of liquefaction and its impact on anchor piles for floating offshore structures. *Soil Dyn. Earthq. Eng.* **127**, 105839 (2019).
8. Wang, D., Merifield, R. & Gaudin, C. Uplift behaviour of helical anchors in clay. *Can. Geotech. J.* **50**, 575–584 (2013).
9. Kwon, O., Lee, J., Kim, G., Kim, I. & Lee, J. Investigation of pullout load capacity for helical anchors subjected to inclined loading conditions using coupled eulerian-lagrangian analyses. *Comput. Geotech.* **111**, 66–75 (2019).
10. Yi, J. T. *et al.* Pull-out capacity of an inclined embedded torpedo anchor subjected to combined vertical and horizontal loading. *Comput. Geotech.* **121**, 103478 (2020).
11. Cerfontaine, B., Knappett, J., Brown, M. J., Davidson, C. & Sharif, Y. Optimised design of screw anchors in tension in sand for renewable energy applications. *Ocean. Eng.* **217**, 108010 (2020).
12. Ayothiraman, R. & Reddy, K. M. Model experiments on pile behaviour in loose-medium dense sand under combined uplift and lateral loads. In *Tunneling and Underground Construction*, 633–643 (2014).
13. Madhusudan Reddy, K. & Ayothiraman, R. Experimental studies on behavior of single pile under combined uplift and lateral loading. *J. Geotech. Geoenvironmental Eng.* **141**, 04015030 (2015).
14. Conte, E., Troncone, A. & Vena, M. Behaviour of flexible piles subjected to inclined loads. *Comput. Geotech.* **69**, 199–209 (2015).
15. Lu, W. & Zhang, G. Influence mechanism of vertical-horizontal combined loads on the response of a single pile in sand. *Soils foundations* **58**, 1228–1239 (2018).
16. Achmus, M. & Thieken, K. On the behavior of piles in non-cohesive soil under combined horizontal and vertical loading. *Acta Geotech.* **5**, 199–210 (2010).
17. Shin, E., Das, B., Puri, V., Yen, S. & Cook, E. Ultimate uplift capacity of model rigid metal piles in clay. *Geotech. & Geol. Eng.* **11**, 203–215 (1993).
18. Ming-hui, Y., Xue-wen, Y. & Ming-hua, Z. Study of model experiments on uplift piles in clay under oblique loads. *J. Hunan Univ. Nat. Sci.* **43** (2016).
19. Bhardwaj, S. & Singh, S. Influence of load obliquity on pullout capacity of micropile in sand. *Indian Geotech. J.* **45**, 200–208 (2015).

20. Ramadan, M. I., Butt, S. D. & Popescu, R. Offshore anchor piles under mooring forces: centrifuge modeling. *Can. geotechnical journal* **50**, 373–381 (2013).

21. Ramadan, M. I., Butt, S. D. & Popescu, R. Offshore anchor piles under mooring forces: numerical modeling. *Can. geotechnical journal* **50**, 189–199 (2013).

22. Hu, C.-b., Mei, L., Mei, G. & ZAI, J.-m. Finite element method for selecting the soil boundary in the model of pile-soil. *Build. Sci.* **9** (2009).

23. Saravanan, R., Arumairaj, P. & Subramani, T. A study on behavior of vertical pile in sand under uplift load. *Geotech. Eng. (SEAGS & AGSSEA)* **49**, 67–72 (2018).

24. Sedov, L. I. *Similarity and dimensional methods in mechanics* (CRC press, 1993).

25. Bhardwaj, S. & Singh, S. Pile capacity under oblique loads–evaluation from load–displacement curves. *Int. J. Geotech. Eng.* **9**, 341–347 (2015).

26. Qiu, Y., Gao, Y. F., Bing, L. I., Wang, Y. K. & Di, W. U. Calculation methods for ultimate inclined bearing capacity of caisson foundation under inclined load. *J. Yangtze River entific Res. Inst.* (2017).

27. Renpeng, K. L. J. L. C. & Yunmin, F. J. L. G. C. Response of squeezed branch piles under inclined uplift loads. *Chin. J. Appl. Mech.* 02 (2013).

28. Gao, Y. *et al.* Experimental studies on the anti-uplift behavior of the suction caissons in sand. *Appl. Ocean. Res.* **43**, 37–45 (2013).

29. WEN, S.-l. & WANG, X.-b. Numerical simulation on the impact of loading angle on the bearing characteristics of pile under the inclined load. *Build. Sci.* S1 (2012).

30. Al-Mhaidib, A. I. & Edil, T. B. Model tests for uplift resistance of piles in sand. *Geotech. Test. J.* **21**, 213–221 (1998).

31. Wang, H., Wang, L., Hong, Y., He, B. & Zhu, R. Quantifying the influence of pile diameter on the load transfer curves of laterally loaded monopile in sand. *Appl. Ocean. Res.* **101**, 102196 (2020).

32. Rahman, M. A. & Sengupta, S. Uplift capacity of inclined underreamed piles subjected to vertical load. *J. Inst. Eng. (India): Ser. A* **98**, 533–544 (2017).

33. Sharma, A. & Sharma, R. K. Uplift behaviour of axial granular pile anchor encased with geogrid in cohesionless soil. *J. Eng. Des. Technol.* (2020).

34. Ai, Z. Y., Zhao, Y. Z. & Cheng, Y. C. Time-dependent response of laterally loaded piles and pile groups embedded in transversely isotropic saturated viscoelastic soils. *Comput. Geotech.* **128**, 103815 (2020).

35. Gaaver & Khaled, E. Uplift capacity of single piles and pile groups embedded in cohesionless soil. *Alex. Eng. J.* **52**, 365–372 (2013).

36. Emirler, B., Tolun, M. & Yildiz, A. 3d numerical response of a single pile under uplift loading embedded in sand. *Geotech. Geol. Eng.* **37**, 4351–4363 (2019).

37. Jamnejad, G. & Hesar, M. A. Stability of pile anchors in the offshore environment. (1995).